Journal of Archaeological Science: Reports 41 (2022) 103315

Contents lists available at ScienceDirect

Journal of Archaeological Science: Reports

journal homepage: www.elsevier.com/locate/jasrep

Comparing three sample preparation techniques for portable X-ray fluorescence: A case study of Coarse Orange ceramic jars, Veracruz, Mexico

Marc D. Marino [a,*], Wesley D. Stoner [a], Lane F. Fargher [b], Michael D. Glascock [c]

[a] Department of Anthropology, 330 Old Main, University of Arkansas, Fayetteville, AR 72704, United States
[b] Departamento de Ecología Humana, Centro de Investigación y de Estudios Avanzados del IPN – Unidad Mérida, km 6 carretera Antigua a Progreso, Col. Cordemex, Mérida, YUC C.P. 97310, Mexico
[c] Research Reactor Center, University of Missouri, 1513 Research Park Dr. Columbia, MO 65211, United States

ARTICLE INFO

Keywords:
pXRF
Ceramics
Archaeology
Trade
Exchange

ABSTRACT

Applications of energy dispersive portable X-ray fluorescence (pXRF; Olympus Vanta M Series VMR) for the chemical analysis of ceramic fabrics are gaining importance for archaeology. In addition to the broad accessibility of the instruments and their ability to gain first-look chemical data without destroying archaeological samples, the ability to bring the instrument to the field may be the only option for researchers working internationally. Through a systematic evaluation of quality control measures applied to multiple standard and in-house reference materials, we conclude that the pXRF employed in this study can precisely and accurately quantify many elements, some of which are not reported or possess high detection limits as measured by other instruments, including neutron activation analysis (NAA). We also demonstrate that analyzing ceramics in different states – intact sherds, homogenized powders, or pressed planchets – produce internally consistent results within categories but yield different results across sample preparation techniques. Finally, we re-analyze an archaeological sample of Coarse Orange jars from the Classic period Tuxtla Mountains, Veracruz, Mexico previously studied through petrography and NAA (Stoner, 2013; Stoner et al., 2008). Analyses of samples processed into homogenized powders yield the most accurate and precise results, rivaling the analytical capabilities of NAA for characterizing this particular sample of ceramics. Analysis of intact sherds and pressed planchets yields sufficient results to reproduce the main compositional groups identified through prior NAA, but loses some detail necessary to separate subgroups.

1. Introduction

Archaeologists and material scientists employ chemical analysis of ceramics to identify exchange relationships, raw material procurement strategies, and production processes of the past (Arnold, 2000; Arnold et al., 1991; Bishop, 1980; Neff et al., 1988; Stoner and Glascock, 2012; Weigand et al., 1977; Sayre and Harbottle, 1979). Instrumental techniques, typically housed at universities, have been developed to this end, including neutron activation analysis (NAA), inductively coupled plasma – mass spectrometry (ICP-MS), or energy dispersive X-ray fluorescence (ED-XRF). In cases of international research, samples are often exported, which can be a lengthy process with many countries limiting the number of specimens or prohibiting export entirely. In those cases, the ability to bring the instrument to the field, such as with portable X-ray fluorescence, may enable research that would otherwise be impossible (see Aimers et al., 2011; Scott et al., 2018; Xu et al., 2019). Further, in cases where NAA or another technique is applied, pXRF provides a quick way to generate first-look data useful for staged sampling procedures that can more effectively target the best sample to answer archaeological questions. Partly due to its ease of use, procedures for the application of pXRF to the study of archaeological ceramics have been applied in non-standardized ways. The proliferation of casual applications of pXRF creates data islands that do little to advance archaeological science (Speakman and Shackley, 2013). We focus our efforts to establish systematic calibration and sample preparation procedures using an Olympus Vanta M series VMR pXRF.

In this study, we use pXRF to run multiple replicates of reference materials and archaeological samples prepared into different sample states. These include standard reference materials (SRMs) with certified, reference, and information values (see May et al., 2000 for definitions of

* Corresponding author.
E-mail address: mdmarino@uark.edu (M.D. Marino).

https://doi.org/10.1016/j.jasrep.2021.103315
Received 11 October 2021; Received in revised form 5 December 2021; Accepted 6 December 2021
Available online 21 December 2021

Table 1
Reference materials (n = 24) used to correct and test the Olympus Vanta pXRF calibration for 17 elements.

Name	Type	Matrix	Used For:
SRM1645*	Sediment	Planchet	Correction
SRM2709*	Soil	Planchet	Correction
SRM97b*	Clay	Planchet	Correction
SARM46**	Clay	Planchet	Correction
SARM52**	Sediment	Planchet	Correction
SARM69**	Pottery	Planchet	Correction
OM4 Ball Clay***	Clay	Planchet	Correction
Pikermi***	Clay	Planchet	Correction
Talc Free***	Clay	Planchet	Correction
Albany Clay***	Clay	Planchet/ Powder	Planchet Correction & Asses Powder LDR
Alberta Clay***	Clay	Planchet/ Powder	Planchet Correction & Asses Powder LDR
Cornwall Clay***	Clay	Planchet/ Powder	Planchet Correction & Asses Powder LDR
Ohio Gold Clay***	Clay	Planchet/ Powder	Planchet Correction & Asses Powder LDR
Red Art 2000***	Clay	Pellet/ Powder	Correction
Red Art***	Clay	Planchet/ Powder	Correction
SRM2711*	Soil	Planchet/ Powder	Powder Correction & Test Planchet Correction
SRM679*	Clay	Pellet/ Powder	Correction
SRM2711a*	Soil	Powder	Test Powder Correction
Barnard Clay***	Clay	Powder	Assess Powder LDR
Bentonite + 25% CaO***	Clay + Oxide	Powder	Assess Powder LDR
Bentonite Clay***	Clay	Powder	Powder Correction
CaO***	Oxide	Powder	Assess Powder LDR
Hawthorne Clay***	Clay	Powder	Assess Powder LDR
PV Clay***	Clay	Powder	Assess Powder LDR

* NIST Standard Reference Materials.
** South African Reference Materials.
*** MURR Secondary Reference Materials.
List of 17 elements used to correct the Olympus Vanta PXRF: Aluminum (Al), Silicon (Si), Potassium (K), Calcium (Ca), Titanium (Ti), Chromium (Cr), Manganese (Mn), Iron (Fe), Nickel (Ni), Copper (Cu), Zinc (Zn), Rubidium (Rb), Strontium (Sr), Yttrium (Y), Zirconium (Zr), Niobium (Nb), Lead (Pb).

standard, reference, and information values), secondary reference materials that were prepared by the University of Missouri Research Reactor (MURR) (see JCGM, 2012:48)[1]; and archaeological ceramics[2] previously characterized via NAA and petrography (Table 1). We analyze three parallel datasets for the same archaeological samples divided into different sample states (Fig. 1). (1) Intact sherds (archaeological ceramics and reference materials fired into clay pucks) were cleaned with water and the surfaces were burred with an aluminosilicate paper to eliminate surface sediment; (2) homogenized powders were created by first burring the surfaces of sherds, and then grinding them into powders using an agate mortar and pestle; (3) pressed planchets were created from powders created in stage 2, using a binding agent and pellet press[3]. (See Table 2).

Our study indicates that all materials, including reference materials, analyzed in a powdered state yield the most precise and accurate results

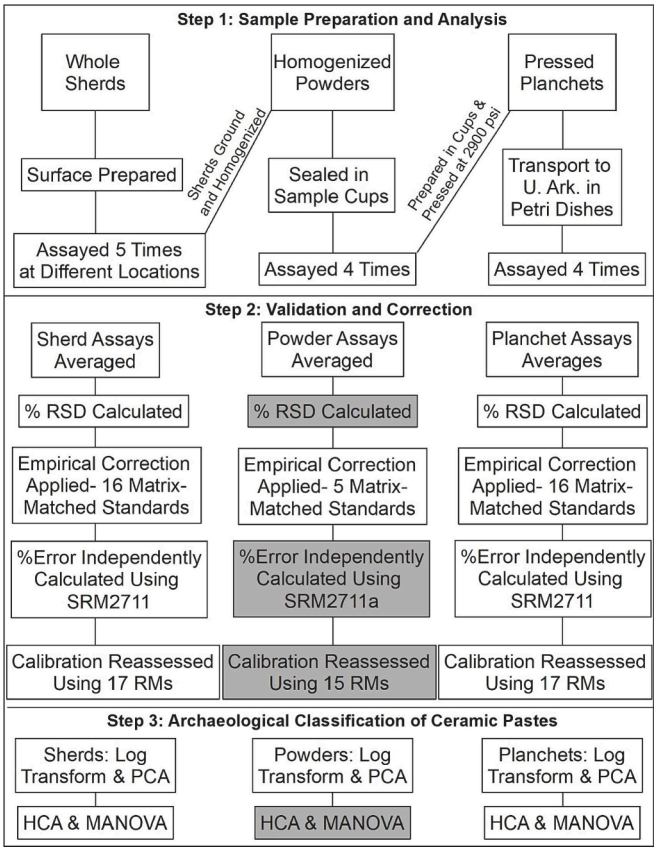

Fig. 1. Workflow of different sample preparation procedures. Grey boxes indicate the lowest %RSD, and the highest accuracy returned.

within material category. Those data closely replicate the results obtained by NAA for many elements and offer superior quantification of other elements that are near or below detection limits of NAA (c.f. LeMoin and Helperin, 2021). Analysis of reference materials as fired pucks and planchets yields lower precision and less accurate results. Analysis of intact archaeological sherds introduces variability due to their coarse textures and the need to average values obtained at different locations to estimate bulk composition. Other analytical factors added variability that were difficult to control: the position of sherds over the detector introduces variability in the angle of the sample and the air gap between sherd and detector. Analysis of archaeological specimens prepared as planchets also yield results with a lower precision than those prepared as powders, possibly due to the calibration of the machine at the factory with powder reference materials. With these cautions in mind, our methodological contribution to the application of pXRF demonstrates that it is a viable, independent method for elemental quantification of archaeological ceramics from the Tuxtla Mountains, Veracruz, Mexico. For more detailed compositional analyses, a small piece of the sherd should be homogenized into a powder. Alternatively, initial sample screening and coarse grouping procedures can be met by averaged assays over a cleaned and intact sherd.

2. Benefits and limitations of PXRF for analysis of ceramics fabrics

The benefits of pXRF are numerous: (1) the instruments have become widely available and affordable for purchase by archaeological researchers; (2) the primary benefit of pXRF in the hands of an archaeologist is to conduct first-look data in the field, guiding research and sampling strategies in real time. Large research labs may not dedicate time and resources to such preliminary data collection, and dealing with

[1] Where we use the general term "reference materials" we refer to SRMs and secondary reference materials together. For a complete list of color-coded reference material sources, values, and links, see Supplemental Materials 2.
[2] All archaeological ceramics were previously permitted for permanent export for destructive analysis by the Instituto Nacional de Antropología e Historia, Mexico (Stoner 2002, 2011).
[3] Where we use the short term "sherds", "powders", and "planchets", that refers to intact sherds, homogenized powders, and pressed planchet samples, respectively.

Table 2
Lower limit of detection (LLOD) and linear dynamic range (LDR) for powdered and planchet reference materials and CO samples. Upper LDR values represent the highest concentrations observed in the available standards.

Element	LoD for Olympus†	Powdered RMs	LDR Based on Powder RMs	LDR CO (Powder)	Planchet RMs	LDR Based on Planchets RMs	LDR CO (Planchets)
N = 34	LLoD (ppm)	LLoD (ppm)	LDR (ppm)	LDR (ppm)	LLoD (ppm)	LDR (ppm)	LDR (ppm)
Mg	<3000	<2844	9385–32157	***	<2614	8626 – 21,537	***
Al	<400	<20911*	69008–168528	74192–158867	<6906*	22792–189342	71414–150642
Si	<400	<53593*	176857–335665	178468–264427	<39388*	129981–338666	199304–317955
P	<50	<39	130 – 867	***	<60*	199 – 1899	***
S	<50	<78	258–3336	**	<19	64 – 20,739	**
K	<25	<18	61–74105	6851–18565	<157*	520 – 42,912	7598–21834
Ca	<25	<552*	2013–415378	4237–85567	<345*	1140–112677	2070–88567
Ti	<25	<57*	190–11785	4392–7243	<918*	3031 – 12,738	4380 – 7519
V	<25	<39*	131 – 415	***	<11	38 – 268	***
Cr	<10	<9	32 – 251****	98–596	<15	47 – 33,896	86 – 652
Mn	<5	<14*	47–51513	200–951	<8	28 – 8840	182 – 996
Fe	<5	<315*	1040 – (92440)	26501–63135	<330*	991 – 194,418	26504–71280
Co	<5	**			**		
Ni	<5	<5	15 – 125****	56–303	<5	15 – 172	50 – 320
Cu	<10	<2	7 – 111	14–47	<3	10 – 479	14 – 48
Zn	<5	<1	5 – 396	68–151	<2	5 – 6997	71 – 159
As	<5	<1	6 – 81	**	<2	7 – 488	**
Se	<5	**			**		
Rb	<5	<1	3 – 505	30–108	<6	21 – 466	30 – 107
Sr	<5	<10*	35 – 790	84–436	<7	23 – 749	87 – 452
Y	<5	<1	3 – 54	16–28	<2	5 – 61	14 – 26
Zr	<5	<5	18 – 333	114–217	<5	16 – 410	95 – 215
Nb	<5	<2	6 – 29	10–18	<2	6–46.1	11 – 18
Mo	<5	<2	6 – 115	**	<2	6 – 13	**
Ag	<5	**			**		
Cd	<5	**			**		
Sn	<5	**			**		
Sb	<5	**			**		
W	<5	**			**		
Hg	<5	**			**		
Pb	<5	<9	30 – 1384	5–19	<5	15 – 14,287	5–19
Bi	<5	**			**		
Th	<5	<2	8 – 37	***	<4	13 – 38	***
U	<5	**			**		

* Actual LLoD lower than the calculated LLoD using reference materials.
** Concentrations are too low to reach LLoD or LLoQ.
*** Typical clay/sediment concentrations in SRMs are too low to create appropriate calibration needed to estimate the LDR of Coarse Orange archaeological samples.
****NAA values of Coarse Orange Samples used to corroborate LDR due to low concentrations in SRMs.
† https://www.olympus-ims.com/en/downloads/detail/?0%5bdownloads%5d%5bid%5d=276827648.

transport, permits, and delays to work up data can prolong decisions that archaeologists need to make quickly during short field seasons; (3) the ability to conduct analyses near project sites expedite research flows, and, in some cases, might be the only way to collect chemical data due to export restrictions or prohibition over destructive analyses. A great example of this is the recent pXRF analysis of Emperor Qin Shihuang's *terracotta* army (Quinn et al., 2020). (4) Related, is the ability to conduct non-destructive analysis, but we caution that analysis of intact sherds carries a number of significant drawbacks that limit the utility of the data.

Sample preparation has a dramatic effect on the measurement of bulk chemical composition with any instrumentation. X-ray fluorescence is sensitive to variations in sample texture, compaction, homogeneity, surface topography, and position of the sample relative to the detector (Forster et al., 2011; McCormick and Wells, 2014). Further, ceramics fabrics are often inhomogeneous materials with compositional variation deriving from diverse inputs, including the materials used (water, clay, natural aplastics, tempering materials), use, and post-depositional chemical changes (Arnold, 2000; Arnold et al., 1991; Carpenter and Feinman, 1999; Golitko et al., 2012; Neff et al., 1988; Stoner, 2016; Stoner and Shaulis, 2021). Additionally, foreign particulates can cling to the surfaces and invade the pores of pottery. Without a standard protocol for processing samples and evaluating the results, the numbers that result from the application of any chemical technique might represent compositions that were not part of the original paste recipe.

If a fabric analysis is desired, eliminating surface "contaminants" – dirt, slips, paints, glazes – must be done through burring or abrading (Aimers et al., 2011; Glascock, 1992; Neff, 2000; Glascock & Neff, 2003). X-rays excite atoms at different depths into the material, up to several mm into the sample depending on their energies (Shackley, 2011), with surface adherents included in the resulting data if not removed. Diagenetic chemical changes, however, can penetrate deep into the ceramic body such that even deep burring cannot remove all traces (Stoner and Shaulis, 2021). Another unknown is whether surface burring drives surface contaminants deeper into the ceramic bodies. Other sample extraction techniques might be better in this respect, such as drilling powders from the broken edges of sherds (Blackman and Bishop, 2007:324), but the use of metal drill bits also can introduce contaminants (Boulanger et al., 2012).

Potters around the world often added materials to temper the fabric, particularly when using clays with high swell-shrink ratios that lead to high percentages of breakage upon firing. Aplastic particles halt crack propagation, enhancing the pot's resistance to thermal and mechanical shock, and taking up volume within so they do not shrink as much with water loss (Arnold, 1985:23; Rye, 1981:27). Unless the chemistries of individual components of the ceramic paste are sought (Stoner, 2016), the ceramic fabric must be homogenized into a fine power, or in the case of pXRF, sherds analyzed at multiple locations to approximate the bulk chemical composition. If the tempering materials themselves are inhomogeneous in composition or texture, analysis of different parts of the same sherd may result in very different data. Naturally gritty/sandy clays present the same issues as tempered ceramics if not homogenized during sample preparation.

Table 3
Relative standard deviation (%RSD) among the four overlapping reference materials prepared as homogenized-powders and pressed-planchets used for correction.

	SRM679 %RSD	SRM 679 %RSD	OR %RSD	OR %RSD	NOR %RSD	NOR %RSD	SRM2711 %RSD	SRM2711 %RSD
Elem.	Powder	Planchet	Powder	Planchet	Powder	Planchet	Powder	Planchet
n=34	n=16	n=16	n=12	n=10	n=17	n=11	n=11	n=15
Mg	<LOD	<LOD	<LOD	<LOD	<LOD	<LOD	17.33	15.13
Al	1.44	1.51	1.82	0.55	1.26	2.03	0.75	0.57
Si	2.28	1.65	0.88	0.68	0.87	3.46	0.48	0.32
P	3.66	7.27	<LOD	<LOD	14.93	23.18	2.58	3.27
S	20.83	24.61	15.86	6.52	<LOD	<LOD	2.03	1.45
K	1.46	1.19	1.17	0.36	1.00	2.60	0.31	0.79
Ca	<LOD	<LOD	<LOD	<LOD	<LOD	<LOD	0.81	1.33
Ti	0.91	0.89	0.92	0.91	1.15	2.33	1.65	0.98
V	5.40	4.52	2.38	3.88	4.44	4.03	5.25	4.24
Cr	7.40	8.77	5.92	6.71	7.96	4.44	10.24	9.36
Mn	1.08	1.09	2.36	2.80	2.43	1.32	1.16	1.27
Fe	0.54	0.80	0.38	0.56	0.97	0.72	0.75	0.42
Co	<LOD	<LOD	<LOD	<LOD	<LOD	<LOD	<LOD	<LOD
Ni	5.63	4.34	3.30	4.61	3.43	2.50	5.92	9.49
Cu	3.76	5.08	4.67	4.55	6.28	4.42	1.79	1.47
Zn	1.23	0.85	1.45	1.22	1.82	1.82	1.20	0.92
As	6.02	4.07	3.07	4.03	3.74	3.27	4.33	4.29
Se	<LOD	<LOD	<LOD	<LOD	<LOD	<LOD	27.04	27.64
Rb	0.48	0.57	0.53	0.49	0.50	0.62	0.68	0.75
Sr	0.93	0.64	1.20	0.82	1.14	1.31	0.56	0.44
Y	1.41	1.59	1.74	1.46	1.83	1.87	2.07	1.68
Zr	0.57	0.32	1.35	0.64	1.24	1.26	0.51	1.01
Nb	2.10	3.37	2.86	2.39	2.26	4.71	2.99	2.34
Mo	7.44	17.07	<LOD	<LOD	<LOD	<LOD	<LOD	<LOD
Ag	<LOD	<LOD	<LOD	<LOD	<LOD	<LOD	<LOD	<LOD
Cd	<LOD	<LOD	<LOD	<LOD	<LOD	<LOD	5.00	9.65
Sn	<LOD	<LOD	<LOD	<LOD	<LOD	<LOD	<LOD	<LOD
Sb	<LOD	<LOD	<LOD	<LOD	<LOD	<LOD	7.29	14.42
W	<LOD	<LOD	14.61	38.21	18.35	18.66	<LOD	<LOD
Hg	16.92	14.55	13.96	11.23	14.58	13.76	5.79	8.43
Pb	3.76	3.18	3.76	5.05	4.24	5.96	0.31	0.49
Th	5.55	5.96	5.76	8.91	7.40	22.91	8.37	7.07
U	<LOD	<LOD	<LOD	<LOD	<LOD	<LOD	<LOD	<LOD
Near 10%	21	20	19	19	19	18	25	24

The positioning and shape of the analyzed surface can also generate variability not directly reflective of the material composition, and irregular surface topography can attenuate incident or fluorescent x-rays (Aimers et al., 2011; Desroches et al., 2018). Spacing of the incident x-rays from sample to the detector directly co-varies with fluctuations in the rate of returning photons, so an irregularly shaped sample will return different compositions from different parts of the sherd. Irregularly shaped samples, as is the case with most sherds, are difficult to position consistently in relation to the detector.

Quantifications using unassessed factory pXRF calibrations are also problematic. Factory calibrations typically focus on quantifying heavier elements or metals associated with industrial or environmental issues (Hu et al., 2017; Hunt and Speakman, 2015; Jang, 2010). Higher voltage is required to fluoresce heavier elements, while lower voltage is appropriate for lighter elements occurring at greater concentrations in aluminosilicate clays. Calibrations focusing on heavier elements, or metals, may misrepresent or miss lighter elements (Lemier, 2018). Some light elements require a vacuum or helium atmosphere, and custom calibrations or empirical corrections, using multiple reference materials, are appropriate for archaeological ceramics (Johnson, 2014).

Standardization errors are also introduced if standards and samples are not 'matrix-matched.' To limit such errors, the crystalline structures and chemistries found within reference materials and 'unknowns' should be similar (Aimers et al., 2011). Matrix-matching requires the particle size of both unknowns and reference materials be ground to < 50 μm. We used soil, sediment, and clay reference materials occupying a range of elemental concentrations.

Table 4
Validation of elements (in grey) for planchet SRM271, powder SRM2711a, and NAA SRM2711.

	SRM 2711 (Planchet)				SRM2711a (Powder)				SRM2711 (NAA)				SRM2711 (NIST)		SRM2711a (NIST)	
Elem.	2711 PPM	SD	% RSD	% Error	2711a PPM	SD	% RSD	% Error	2711 PPM	SD	% RSD	% Error	2711 PPM	SD	2711a PPM	SD
Mg	5187.1	769	15.13	50.6	8498.99	702	17.33	20.57	--	--	--	--	10500	300	10700	600
Al	64697.85	400	0.57	0.92	69625.33	478	0.75	3.61	70522.15	1006.8	3.19	7.99	65300	900	67200	600
Si	317481.5	950	0.32	4.3	284943.3	1312	0.48	9.25	--	--	--	--	304400	1900	314000	7000
P	1055.78	23	3.27	22.77	1001.42	22	2.58	18.93	--	--	--	--	860	70	842	11
S	1007.87	16	1.45	139.97	1110.74	31	2.03	--	--	--	--	--	420	10	--	--
K	25914.41	177	0.79	5.77	23375.63	73	0.31	7.61	24500	947.74	7.75	11.55	24500	800	25300	1000
Ca	29890.1	365	1.33	3.79	24837.35	189	0.81	2.63	30645.84	279.67	2.04	6.41	28800	800	24200	600
Ti	3031.04	31	0.98	0.95	3015.62	56	1.65	4.87	3208.46	155.3	10.82	4.85	3060	230	3170	80
V	116.61	3	4.24	42.21	127.27	4.6	5.25	57.7	91.06	2.67	6.56	11.05	81.6	2.9	80.7	5.7
Cr	49.78	3.75	9.36	5.91	55.88	4.3	10.24	6.85	49.92	0.4	1.81	6.21	47	--	52.3	2.9
Mn	612.89	7.88	1.27	3.94	620.49	7.6	1.16	8.08	722.42	3.01	0.93	13.23	638	28	675	18
Fe	27895.37	112	0.42	3.48	26920.45	202	0.75	4.54	31242.6	305.1	2.18	8.11	28900	600	28200	400
Co	0	<LOD	<LOD	100	0	<LOD	<LOD	100	10.48	0.17	1.63	4.84	10	--	9.89	0.18
Ni	19.75	1.86	9.49	4.15	24.63	1.5	5.92	13.5	6.72	9.22	137.13	67.37	20.6	1.1	21.7	0.7
Cu	101.54	1.71	1.47	10.93	149.73	2.6	1.79	6.95	--	--	--	--	114	2	140	2
Zn	384.8	3.19	0.92	9.94	396.68	5.1	1.2	4.18	356.88	21.58	6.05	1.97	350.4	4.8	414	11
As	59.87	2.39	4.29	42.98	57.46	2.6	4.33	46.3	105.75	0.74	0.7	0.71	105	8	107	5
Se	2.49	0.53	27.64	63.68	1.73	0.46	27.04	--	--	--	--	--	1.52	0.14	2	
Rb	114.96	0.83	0.75	4.51	116.79	0.81	0.68	2.67	122.11	4.24	3.47	11.01	110	--	120	3
Sr	226.78	1.02	0.44	7.44	229.64	1.28	0.56	5.11	258.19	39.04	15.12	5.38	245.3	0.7	242	10
Y	28.58	0.61	1.68	14.3	30.34	0.82	2.07	8.06	--	--	--	--	25	--	--	--
Zr	246.76	2.62	1.01	7.29	222.57	1.49	0.51	--	213.27	22.11	10.37	7.27	230	--	--	--
Nb	18.01	0.42	2.34	--	13.85	0.6	2.99	--	--	--	--	--	--	--	--	--
Mo	0	<LOD	<LOD	100	0.36	<LOD	<LOD	79.1	--	--	--	--	1.6	--	--	--
Ag	0	<LOD	<LOD	100	0	<LOD	<LOD	100	--	--	--	--	4.63	--	--	--
Cd	37.63	3.34	9.65	9.76	49	2.4	5	3.29	--	--	--	--	41.7	0.25	54.1	0.5
Sn	0.71	2.67	<LOD	--	8.45	<LOD	<LOD	--	--	--	--	--	--	--	--	--
Sb	26.87	3.79	14.42	38.51	37.18	2.87	7.29	56.22	19.99	0.47	2.33	3.03	19.4	1.8	23.8	1.4
W	3.91	3.13	<LOD	30.21	4.67	2.81	<LOD	51.99	--	--	--	--	3	--	--	--
Hg	7.65	0.77	8.43	22.36	14.92	0.67	5.79	138.7	--	--	--	--	--	--	--	--
Pb	1228.56	5.85	0.49	5.73	1384.56	4.76	0.31	1.1	--	--	--	--	1162	31	1400	10
Bi	0	<LOD	<LOD	--	0.91	2.02	8.37	--	--	--	--	--	--	--	--	--
Th	13.05	<LOD	<LOD	6.8	8.91	<LOD	<LOD	40.59	14.36	0.41	2.86	2.6	14	--	15	1
U	2.97	<LOD	<LOD	14.25	3.39	<LOD	<LOD	12.68	3.16	0.33	10.52	21.51	2.6	--	--	--

Table 5
Breakdown of elements detected by the Olympus Vanta pXRF, NAA, and elements used for chemical group characterization in this analysis of the Coarse Orange dataset.

Elements analyzed by Vanta pXRF (N = 34)	Mg, Al, Si, P, S, K, Ca, Ti, V, Cr, Mn, Fe, Co, Ni, Cu, Zn, As, Se, Rb, Sr, Y, Zr, Nb, Mo, Ag, Cd, Sn, Sb, W, Hg, Pb, Bi, Th, U
Elements analyzed by NAA (N = 33)	As, La, Lu, Nd, Sm, U, Yb, Ce, Co, Cr, Cs, Eu, Fe, Hf, Ni, Rb, Sb, Sc, Sr, Ta, Tb, Th, Zn, Zr, Al, Ba, Ca, Dy, K, Mn, Na, Ti, V
Overlapping elements Analyzed by pXRF and NAA (N = 18)	Al, K, Ca, Ti, V, Cr, Mn, Fe, Co, Ni, Zn, As, Rb, Sr, Sb, Zr, Th, U
Elements used in NAA classification in this paper (N = 29), As, U, Ba, Zn removed	La, Lu, Nd, Sm, Yb, Ce, Co, Cr, Cs, Eu, Fe, Hf, Ni, Rb, Sb, Sc, Sr, Ta, Tb, Th, Zr, Al, Ca, Dy, K, Mn, Na, T, V
Elements near 10% RSD in Sherds, Powders, Planchets (except Th in sherds and planchets) (N = 20)	Al, Si, P, K, Ca, Ti, V, Cr, Mn, Fe, Ni, Cu, Zn, Rb, Sr, Y, Zr, Nb, Pb, Th
Validated pXRF elements used in group characterization (near 10% RSD, <20% Error) (N = 17)	Al, Si, K, Ca, Ti, Cr, Mn, Fe, Ni, Cu, Zn, Rb, Sr, Y, Zr, Nb, Pb
Elements excluded due to narrow range in pXRF SRMs	V, As, Th, U
Elements excluded due to falling below the Limit of Quantification in all samples	Mg, P, Co, S, Se, Mo, Ag, Cd, Sn, Sb, W, Hg, Bi
NAA elements with lower %RSD (5 replicates of SRM2711)	Cr, V, As, Th, Sb
PXRF elements with lower %RSD (10 replicates of SRM2711)	Al, K, Ca, Ti, Mn, Fe, Ni, Zn, Rb, Sr, Zr, U

3. The sample

In this study we use a sample of archaeological ceramics from Veracruz, Mexico as a test of the viability of pXRF to independently construct the same compositional groups previously identified via NAA. Of more generalized interest, though, we analyze a series of reference materials commonly used in instrument calibrations and standardization methods across multiple disciplines.

4. Reference materials

Materials commonly used by multiple laboratories across disciplines are examined here to evaluate: (1) the pXRFs capabilities and limitations for each element; (2) its precision and accuracy compared to reported consensus values; (3) to construct calibration curves to correct the data; and (4) to provide a test of the effects of sample preparation independent from the archaeological ceramics. Concentration values for all reference materials used in this study are transcribed in Glascock (2017; 2020) or GeoReM (http://georem.mpch-mainz.gwdg.de) (see Supplementary Material 3 for all values and citations).

We examine three SRMs as powders, and two common secondary standards that have been widely used across a wide variety of labs and projects. An additional ten secondary and internal standards were assayed as powders (Table 1).

We pressed five SRMs into planchets, as well as two certified standards, and two common secondary standards used across a wide variety of labs and projects. An additional eight secondary standards were assayed as planchets (Table 1).

4.1. Coarse Orange jars in southern Veracruz

Fragments of Coarse Orange jars were recovered at Middle and Late

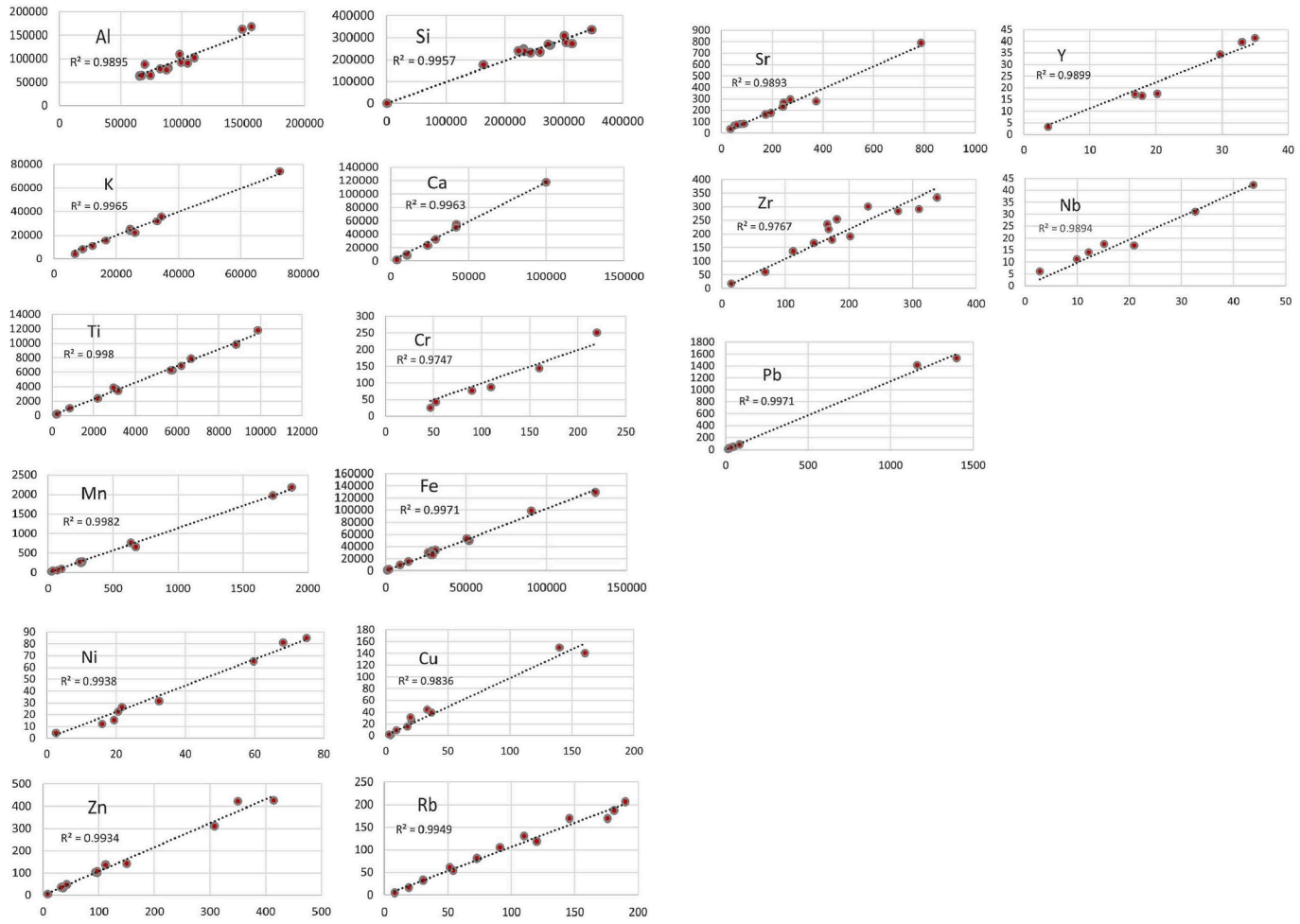

Fig. 2. Regression of powder reference materials (Y-axis) and observed (corrected) values (X-axis) for 17 elements within the Vanta's linear dynamic range, and used to characterize the CO datasets.

Classic Period (A.D. 450–850) sites in the Tuxtla Mountains, Veracruz (Pool, 1990; Santley et al., 1989; Stoner, 2002; 2011; Stoner and Pool, 2015); including the regional center of Matacapan, where it was manufactured most intensively (Arnold et al., 1993; Pool, 1990; Pool and Stoner, 2008; Santley et al., 1989; Stoner, 2013). Coarse Orange pottery factored heavily into the political economy of Matacapan, including the Comoapan production facility where the remains of 36 updraft kilns have been recovered, representing an independent community of specialized potters (Pool, 1990).

Kaolinitic clays of the Concepción formation compose all Coarse Orange jars made in the Tuxtlas. Matacapan potters used clay sources located near the Comoapan production facility and outcrops further south along the Catemaco River that are high in calcium, strontium, and some other elements. Pool (1990) termed these "Group C" clays due to their proximity to Comoapan. They derive from deeper positions in the Concepción formation exposed through incision by the Catemaco River, the largest in the region. In other areas, including the Tepango Valley, the area around Teotepec north of Lake Catemaco, and the southern Tuxtlas Piedmont, Concepción clays display lower concentrations of calcium and strontium, diluted primarily due higher proportions of quartz minerals. Pool (1990) termed these "Group S" clays, after the modern community of Sehualaca, and noted that they derive from the upper Concepción formation closer to the contact with Filisóla quartz and feldspar sands. In these locations, erosion from smaller rivers did not incise as deeply into the Concepción formation. Group S clays also contain higher concentrations of Zr and Hf that derive from zircons commonly associated with quartz sand.

Using NAA, Stoner distinguishes Coarse Orange ceramics made with Group C clays as the CO1 paste recipe (Stoner, 2013). Group CO2 ceramics, low in Ca and Sr, derive from the low-Ca Group S clays. Group CO3 ceramics, primarily recovered near modern Hueyapan de Ocampo in the southern Tuxtla foothills (Killion and Urcid, 2001), also utilized Group S clays but potters tempered those vessels with river sands, a multi-mineral material that includes volcanic ash, rather than bedded volcanic ash. CO3 samples contain lower concentrations of Ca, Fe, and Cr (Pool and Stoner, 2008:415-418).

Volcanic ash was used to temper the paste of all Coarse Orange pots: the ceramic type is partly defined based on presence of these tempering materials. Volcanic ash in the region is on the mafic end of the volcanic compositional range (andesitic basalts), and is rich in Cr, Fe, Sc, and most other transition metals. Minerals encased in black volcanic glass include mainly calcium-rich plagioclase, olivine, and pyroxene (Stoner, 2002). Accordingly, the volume of ash in pottery positively covaries with the concentrations of the elements mentioned above in the bulk chemistry of ceramics. Ceramics made in the attached production facility near the core of Matacapan (Pit 6) contained visibly less volcanic ash than those produced at Comoapan (Pool, 1990; Stoner et al., 2008) and consequently separate as their own group due to lower transition metal concentrations (Stoner, 2013). CO1 ceramics were also subdivided into CO1A, those with relatively high concentrations of Cr and associated transmission metals, and CO1B, those that display subtly lower concentrations on the same chemical axes. CO1B was separated mainly because that composition does not appear at the Comoapan production facility, which was the focus of distributional analysis in the

Table 6
Percent error among the four reference materials prepared as powders and planchets that were used for correction.

Elements	Powder	Planchet	Powder	Planchet	Powder	Planchet	Powder	Planchet
N = 34 Total Elements Collected	NOR %Error	NOR %Error	SRM679 %Error	SRM679 %Error	OR %Error	OR %Error	SRM2711 %Error	SRM2711 %Error
Mg	<LOD	<LOD	<LOD	<LOD	<LOD	<LOD	50.07	50.60
Al	1.28	8.45	0.92	10.12	1.54	8.90	5.68	0.92
Si	0.12	13.82	0.98	20.42	<LOD	<LOD	5.19	4.30
P	57.46	25.70	16.17	34.31	<LOD	<LOD	17.32	22.77
S	<LOD	<LOD	<LOD	<LOD	<LOD	<LOD	<LOD	<LOD
K	3.45	24.38	2.22	17.96	3.87	20.11	3.29	5.77
Ca	<LOD	<LOD	<LOD	<LOD	<LOD	<LOD	19.42	3.79
Ti	2.14	4.04	4.26	5.49	3.04	5.19	6.12	0.95
V	15.09	0.79	19.92	6.83	15.55	14.14	43.15	42.21
Cr	10.06	39.65	2.92	9.99	9.51	7.84	30.49	5.91
Mn	1.72	6.64	7.58	9.06	6.17	2.91	12.51	3.94
Fe	0.58	6.52	2.14	11.50	10.33	1.24	5.03	3.48
Co	<LOD	<LOD	<LOD	<LOD	<LOD	<LOD	<LOD	<LOD
Ni	5.15	17.58	1.21	13.21	<LOD	<LOD	1.71	4.13
Cu	5.04	31.23	1.38	17.34	<LOD	<LOD	6.07	10.93
Zn	2.05	20.81	11.71	0.80	3.35	11.37	12.19	9.94
As	14.43	3.50	17.29	21.66	8.17	16.40	22.75	42.98
Se	<LOD	<LOD	<LOD	<LOD	<LOD	<LOD	72.59	63.82
Rb	1.90	5.07	6.87	10.96	5.14	1.07	16.42	4.51
Sr	7.00	22.68	5.38	5.37	13.58	26.92	5.35	7.44
Y	22.80	23.73	3.68	3.97	<LOD	<LOD	30.42	14.32
Zr	7.41	31.41	12.06	7.85	8.56	34.31	0.03	7.29
Nb	4.53	24.55	4.73	25.30	<LOD	<LOD	<LOD	<LOD
Mo	<LOD	<LOD	<LOD	<LOD	<LOD	<LOD	<LOD	<LOD
Ag	<LOD	<LOD	<LOD	<LOD	<LOD	<LOD	<LOD	<LOD
Cd	<LOD	<LOD	<LOD	<LOD	<LOD	<LOD	<LOD	<LOD
Sn	<LOD	<LOD	<LOD	<LOD	<LOD	<LOD	<LOD	<LOD
Sb	<LOD	<LOD	<LOD	<LOD	<LOD	<LOD	<LOD	<LOD
W	<LOD	<LOD	<LOD	<LOD	<LOD	<LOD	<LOD	<LOD
Hg	<LOD	<LOD	<LOD	<LOD	<LOD	<LOD	<LOD	<LOD
Pb	4.91	11.34	3.28	15.80	<LOD	<LOD	10.20	5.73
Bi	<LOD	<LOD	<LOD	<LOD	<LOD	<LOD	<LOD	<LOD
Th	6.03	14.34	14.71	34.70	20.44	7.98	21.88	6.79
U	21.13	34.53	11.04	79.69	51.56	73.42	96.45	14.23
Sum of elements with lowest %Error	18	3	17	4	8	6	8	15
Sum of 15 elements with lowest %Error	14	0	12	2	5	4	4	11

original study.

Our expectations for the pXRF study are to see separation among chemical groups CO1, CO2, and CO3. Following NAA, we expect that these groups should be distinguishable based on Ca and Sr concentrations, differentiating between Group C and S clays used in their production, and a suite of transition metals which indexes the relative concentrations of volcanic ash to quartz sand in the ceramic fabric (Stoner, 2013). A minority of other elements are also important to differentiate Coarse Orange paste recipes (Pool, 1990).

Silicon, the most direct way to chemically measure the relative concentrations of quartz in the sample, is an axis of chemical variation not reported by NAA but is routinely measured by pXRF. The coarser sand-sized quartz inclusions found in group CO2, and the higher amounts of quartz inclusions found in group CO3, should yield elevated levels of Si and Zr in those groups. Based on petrographic point counting, previous NAA and XRF analysis, and knowledge of the local geology, dilution in the concentration of Ca and other elements that are significant for group differentiation was proposed due to the inclusion of quartz and feldspar sands (Pool, 1990; Stoner et al., 2008). Similarly, the relatively higher proportions of volcanic ash proposed for subgroup CO1A (Stoner, 2013) should reflect lower amounts of Si and Zr, and higher amounts of Cr, in comparison to CO1B pots.

Table 7
Statistical comparison of percent error among the four standard and in-house reference materials using a Paired Samples T-test.

Standard	SRM679	OR	NOR	SRM2711
Comparison	Powder Vs. Planchet	Powder Vs. Planchet	Powder Vs. Planchet	Powder Vs. Planchet
K-S Test for Normality	Normal Distribution	Normal Distribution	Normal Distribution	Normal Distribution
Test for Sample Comparison	Paired-Samples *t*-test	Paired-Samples *t*-test	Paired-Samples *t*-test	Paired-Samples *t*-test
d.f.	19	13	19	26
Test Statistic	$t = 2.08$	$t = 2.16$	$t = 2.08$	$t = 2.05$
p-value	0.01	0.11	0.01	0.04

5. Methods: Sample preparation and data analysis

5.1. Instrumentation and calibration

The Olympus Vanta M series VMR pXRF utilizes a Rh anode X-ray tube. Rhodium tubes more easily excite lighter elements than W or Ag tubes. The Vanta alternates between high and low energy X-ray settings, utilizing 40 keV with 70 μA to fluoresce heavier elements and 10 keV with 90 μA to excite lighter elements.

A 40 mm^2 silicon drift detector measures returning energy, emitted after sample irradiation, as analog pulses proportional to the energy of the characteristic X-ray spectra emitted, and are counted at fixed intervals of eV values called channels. Most pXRFs count between 19 and 21 eV per channel, with the Vanta counting 2048 channels total. The spectral resolution of the Vanta for the Full-Width-at-Half-Maximum of the Kα Fe peak (or the area where x-ray peaks are calculated for a given element) is ~ 140 eV (Frahm, 2017).

A Fundamental Parameters calibration (FP), relying on absorption and attenuation coefficients, is used to calculate intensities as counts-per-second (Thomsen, 2007). A relative rate of intensity is then calculated between an unknown analyte to a standard that has a known concentration for a specific element (Thomsen, 2007). A conversion factor, necessary to multiply photon counts quantified by the FP calibration, to reference materials, is then established to obtain concentrations as ppm. For the Vanta's GeoChem calibration, "dozens of SRMs across a wide geochemical range" are used (Frahm, 2018:24).

Olympus recommends that heterogenous materials, like ceramics, require three standards to correct the GeoChem calibration. Five matrix-matched reference materials were available to construct an empirical correction for the powdered dataset (Table 1); SRM2711a, not used to create the correction factor, was assayed to assess precision and accuracy (see Speakman, 2012:13). To ensure the full range of chemical concentrations in the Coarse Orange dataset could be measured precisely and accurately, 10 more powder reference materials were assayed (Table 1).

For the planchets and sherds, the same five reference materials that had been used for the powders were prepared as planchets. However, it was noted early that this correction produced significantly higher errors in the planchets and sherds datasets. To increase the accuracy of the correction, 16 matrix-matched reference materials were used to create the correction; SRM2711, not used to construct the correction, was used to calculate precision and accuracy.

5.2. Sample preparation and measurement

Archaeological sherds were prepared by removing surface contaminants with an aluminosilicate paper and rinsing with deionized water (Fig. 1). The reference materials and archaeological samples not analyzed as powders and planchets were ground and homogenized into a fine powder with a particle size of < 50 μm, using an agate mortar-and-pestle and sealed into XRF cups with prepared thin-film (Chemplex Prolene 4 μm, 3″). Standards were fired into pucks at 850 °C (SRM679), and 1100 °C (NOR), or pressed into planchets to provide a more homogenous matrix. Archaeological sherds were also prepared into planchets.

Planchets were prepared by pipetting 1 ml of Elvacite® solution into a beaker containing 3 – 5 g sample powder, stirring for 2–3 min using a glass rod, and then pressing in XRF cups at 25,000 psi for sixty seconds. Each use included cleaning preparation materials with acetone and ethyl alcohol.

Time to fluoresce heavy and light elements for all samples was ninety seconds using high and low energy settings. Longer dwell times did not diminish estimated error or improve precision, using a shorter time did produce higher errors among some elements. Intact sherds were assayed five times at different locations, providing replicate values. Powders and planchet-samples were assayed four times. Reference materials were analyzed 10–17 times to calculate an average value and standard deviation to measure instrument precision.

5.3. Empirical Correction and validation

We employ a correction of the factory GeoChem calibration to increase the accuracy of measurements obtained in our analysis of archaeological ceramics. A linear 'empirical' correction was employed for both powder and planchet/fired puck corrections based on repeated assays of reference materials. Matrix-matched powdered reference materials were used to correct the powder dataset, and planchet/fired-puck reference materials were used to correct the sherd and the planchet datasets. Because only two clays were available to create the fired puck standards, 14 reference materials prepared as planchets were used in combination with the fired puck standards to create the linear correction for sherds and planchets (Table 1). A linear equation proved to have the best result for the range of element concentrations in our dataset; other datasets, with varying elemental concentrations, may require a different correction equation.

5.4. Validation methods

To build confidence in the instrument's ability to accurately and precisely quantify a suite of elements useful for addressing archaeological questions involving ceramic compositions, we employ a four-step validation procedure (Taverniers et al., 2004). Step one entails calculating percent relative standard deviation (%RSD) from replicate assays of reference materials, which reflects the machine's ability to obtain similar results (Supplementary Materials 1a). Our analysis included 10 to 16 replicate assays of reference materials. The more consistently the pXRF retrieves the same value over repeated measurements, the lower the reported %RSD, with the lowest %RSD representing the highest precision.

Step two entails determining the lower limit where each element can be precisely quantified, also known as the limit of quantification (LoQ) (Desroches et al., 2018; Thomsen et al., 2003).

Step three occurs by determining the upper LoQ, or the highest chemical value where each element can be precisely quantified. The full chemical range of concentrations that can be precisely quantified for each element, from lower to upper limits, is known as the linear dynamic range (the LDR).

Accuracy is measured in step four by assaying many reference materials as unknowns to determine the calibration range where each element can be accurately quantified.

Determining the LDR, or the numerical range of elemental concentrations that can be precisely quantified, can be calculated in several ways (Desroches et al., 2018; Thomsen et al., 2003). The Eurachem Method, applied here, relies on a calculation of %RSD, because %RSD is a direct measure of precision. Percent RSD values that greatly exceed 10% are considered beyond the machine's ability to quantify precisely, and thus, beyond the machine's limit of quantification (LoQ); this

Table 8
Degree of material variation expressed as %RSD for each chemical group previously identified with NAA. Samples here were analyzed as sherds, powders, and planchets. **Bold**- pXRF has lower %RSD, *Italics*- NAA has lower %RSD.

Element	CO				CO1A				CO1B				CO2			
N = 23	Whole % RSD	Powder % RSD	Planchet % RSD	NAA % RSD	Whole % RSD	Powder % RSD	Planchet % RSD	NAA % RSD	Whole % RSD	Powder % RSD	Planchet % RSD	NAA % RSD	Whole % RSD	Powder % RSD	Planchet % RSD	NAA % RSD
Mg	47.88	44.39	40.91		30.55	22.95	21.47		24.49	31.12	25.77		50.56	64.24	55.33	
Al (pXRF)	*24.14*	*16.23*	*15.06*	15.04	**9.42**	**4.92**	**5.37**	5.77	**8.35**	**4.31**	**3.28**	5.29	**10.46**	**4.74**	**3.27**	5.68
Si	9.14	9.39	9.63		6.72	4.14	5.50		5.97	3.44	3.52		11.03	12.88	12.69	
P	73.66	63.64	67.32		59.26	56.59	59.08		65.05	49.77	48.45		83.28	74.34	76.95	
K (NAA)	*25.43*	*21.60*	*22.38*	21.39	**23.63**	**14.95**	**14.21**	16.61	*19.64*	*12.74*	*14.01*	11.70	*34.42*	*32.57*	*34.10*	26.63
Ca (NAA)	*54.09*	*49.06*	*50.98*	40.60	*23.53*	*16.85*	*19.02*	11.88	*27.87*	*22.93*	*23.90*	19.34	*45.03*	*34.27*	*35.80*	31.42
Ti (pXRF)	**10.44**	**9.74**	**10.51**	11.34	**5.67**	**5.07**	**4.61**	6.55	**4.55**	**7.08**	**6.98**	8.84	**9.48**	**6.35**	**6.72**	4.58
V (NAA)	*16.19*	*16.71*	*18.26*	11.25	*16.82*	*14.76*	*15.07*	6.48	*7.62*	*13.19*	*15.49*	5.01	*16.20*	*18.39*	*20.44*	12.78
Cr (NAA)	**26.31**	**28.65**	**30.24**	28.05	*17.62*	*15.24*	*16.86*	11.52	*26.84*	*17.82*	*19.55*	17.22	**27.46**	**30.40**	**35.81**	31.10
Mn (pXRF)	**21.48**	**20.59**	**21.49**	24.05	**8.03**	**5.87**	**6.21**	7.38	**13.09**	**17.47**	**19.35**	21.69	**29.51**	**25.83**	**27.04**	32.74
Fe (pXRF)	**12.95**	**12.27**	**12.13**	13.24	*4.56*	*4.44*	*4.39*	2.37	**5.24**	**5.33**	**5.54**	5.45	**15.77**	**14.99**	**14.49**	16.06
Ni (pXRF)	**36.82**	**29.31**	**31.27**	44.95	**14.47**	**17.51**	**16.74**	19.75	**41.12**	**18.21**	**19.82**	20.98	**32.99**	**30.49**	**35.23**	43.64
Cu	25.84	19.82	20.71		16.89	10.37	13.66		12.23	16.41	13.76		31.64	25.25	23.88	
Zn (pXRF)	**38.86**	**17.63**	**17.86**	37.23	**43.28**	**15.42**	**16.71**	27.74	**25.22**	**10.19**	**9.65**	9.70	**38.62**	**18.89**	**17.46**	58.46
As (pXRF)	**36.22**	**25.73**	**25.34**	64.00	**42.84**	**28.63**	**29.39**	66.52	**19.62**	**27.62**	**18.59**	52.57	**15.17**	**21.31**	**24.68**	77.17
Rb (pXRF)	**26.37**	**24.57**	**25.09**	25.09	**21.98**	**16.87**	**16.08**	17.95	**18.23**	**17.80**	**19.13**	20.18	*32.53*	*29.69*	*30.19*	29.33
Sr (pXRF)	**33.17**	**31.56**	**31.61**	45.01	**15.27**	**13.59**	**14.57**	16.37	**16.26**	**16.49**	**16.85**	25.04	**17.48**	**16.70**	**16.13**	53.19
Y	13.90	13.87	15.18		10.30	6.49	7.79		8.35	5.69	5.88		18.92	17.32	18.89	
Zr (pXRF)	**13.05**	**14.02**	**16.05**	20.78	**6.65**	**6.46**	**5.92**	14.72	**9.09**	**10.14**	**9.78**	16.62	**10.91**	**10.68**	**13.95**	27.40
Nb	9.06	12.41	9.49		7.24	12.42	5.26		6.79	14.72	10.10		11.96	11.20	13.09	
Hg	40.15	19.63	45.08		16.33	19.03	32.15		13.63	15.61	27.66		63.90	24.73	85.43	
Pb	19.17	18.76	21.57		19.57	19.96	22.25		13.41	9.65	12.14		16.53	10.15	11.26	
Th (NAA)	*26.40*	*16.03*	*25.09*	7.11	*17.27*	*9.44*	*14.22*	6.25	*9.17*	*12.79*	*17.57*	5.74	*29.27*	*14.92*	*17.91*	5.85
Avg	27.86	23.29	25.36		19.04	14.87	15.94		17.47	15.67	15.95		28.40	23.93	27.42	
Avg*	26.79	22.25	23.56	27.27	18.07	12.67	13.29	15.86	16.79	14.27	14.63	16.36	24.35	20.68	22.21	30.40

* Average of Elements Collected with pXRF and NAA only.

Table 9
Regression comparing 42 Coarse Orange sherds obtained with pXRF and NAA (Note intact sherds have smaller R^2 values in all cases).

Elements	Whole Vs NAA	Powder Vs NAA	Planchet Vs NAA
Al	0.6657	0.8801	0.8647
K	0.2995	0.7333	0.7546
Ca	0.9284	0.9422	0.966
Ti	0.4776	0.6191	0.567
V	0.0004	0.00002	0.0004
Cr	0.6565	0.8111	0.7348
Mn	0.6978	0.8364	0.8286
Fe	0.6897	0.7669	0.7704
Ni	0.2388	0.5848	0.5885
Zn	0.295	0.7055	0.6809
Rb	0.746	0.9536	0.9508
Sr	0.8416	0.9056	0.8906
Zr	0.4115	0.4403	0.4576
Th	0.0092	0.0772	0.0486
U	0.112	0.1608	0.7836

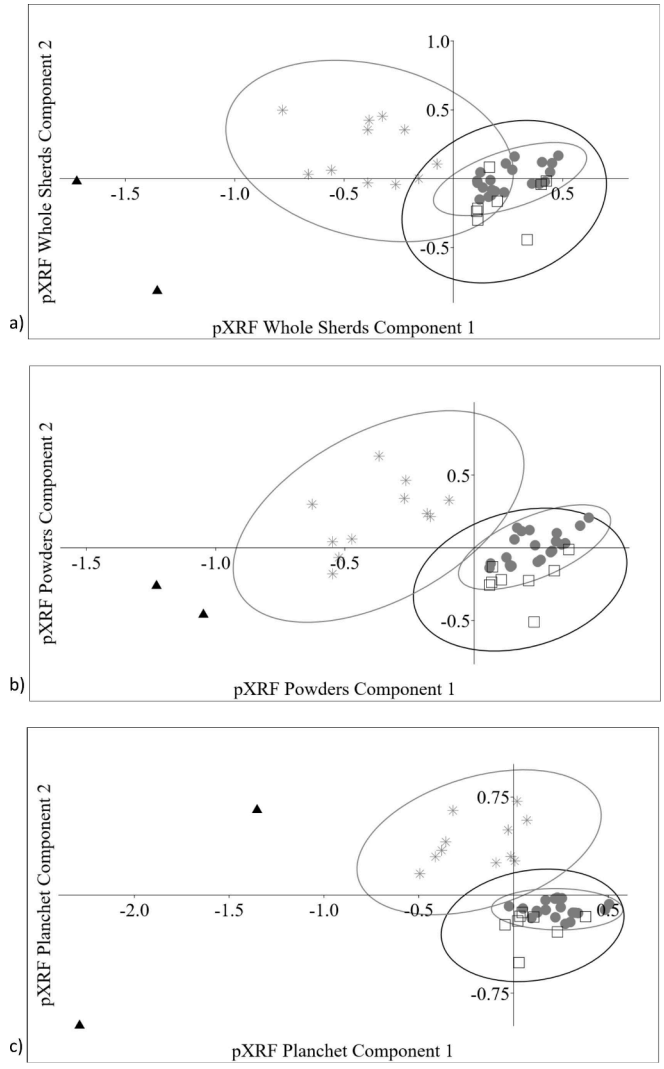

Fig. 3a. Principal components analysis of intact sherds, homogenized powders, and pressed planchets analyzed with pXRF on groups CO1A (Circles), CO1B (Squares), CO2 (Stars), CO3 (Triangles).

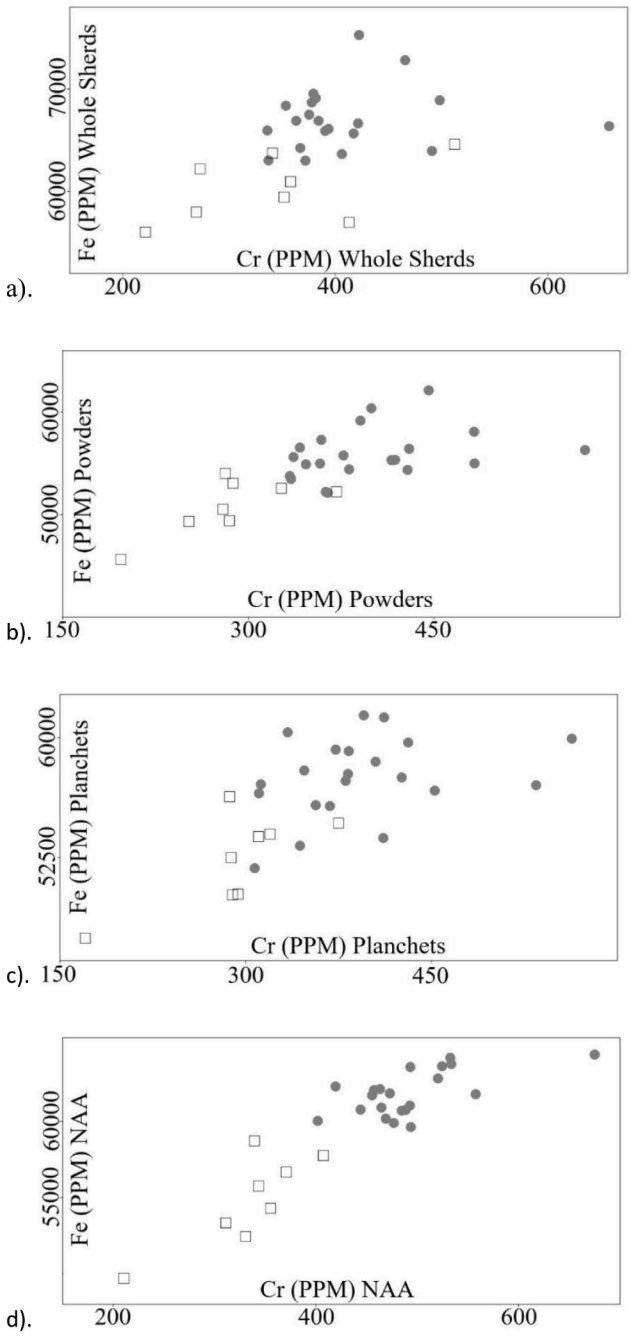

Fig. 4a. Biplot of Cr (X-axis) and Fe (Y-axis) for pXRF data of sherds, powders, planchets, and NAA for sub-groups CO1A (circles) and CO1B (squares).

applies to both the lower and upper LoQ. Percent RSDs in excess of 33% represents the limit of detection (LoD), or the point beyond which the machine can distinguish (detect) an element from background noise (scatter) (Descroches et al., 2018; Thomsen et al., 2003). RSD values above 10% and below 33% can be detected but not precisely quantified.

Step 4, determining accuracy, is calculated as a percentage of the observed error (%Error) between the measured value of each standard, and the actual reported value (Supplementary Materials 1b). The reported values are the certified or information values of the reference materials (Supplementary Materials 2) and the measured values are the averaged replicate values. Only after these measures are used to 'validate' a dataset can results be compared among laboratories with confidence.

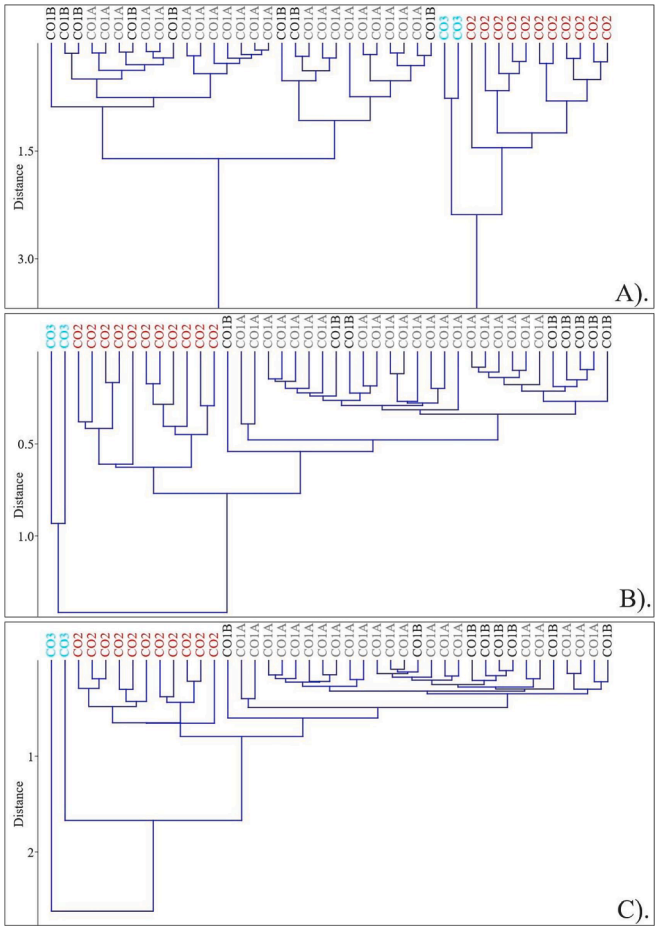

Fig. 5a. Hierarchical cluster analysis of A). intact sherds, B). homogenized powders, and C). pressed planchets, as analyzed with pXRF on groups CO1A, CO1B, CO2, CO3.

5.5. Calculating variation within Coarse Orange chemical groups

After validating the analytical limits of the machine (Table 2), variability within the dataset of archaeological ceramics was assessed by calculating %RSD on the whole dataset and each chemical group as defined previously using NAA.

Variation within each chemical group (CO1A, CO1B, CO2, CO3) was calculated and compared for the different sample preparation techniques (sherds, powders, planchets), and compared to the same measures as calculated among the NAA dataset. As is true with any chemical analysis technique, the 'real' chemical variation that exists in nature for these groups of specimens can only be estimated by instrumental techniques. However, the *relative* variability within chemical groups between the two instruments of variation may indicate the addition of instrumental error of one method over another. Increased analytical imprecision, with all else held equal, will increase variability within any group of unknown samples.

To understand the cause of any observed divergence in variability among groups, a regression analysis was used to compare the compositions of individual archaeological specimens, analyzed as sherds, powders, and planchets, with the corresponding NAA dataset, which was universally analyzed as a homogenized powder. This regression allowed for each sample preparation technique to be assessed independently, useful for corroborating whether variation was added in the form of instrumental error.

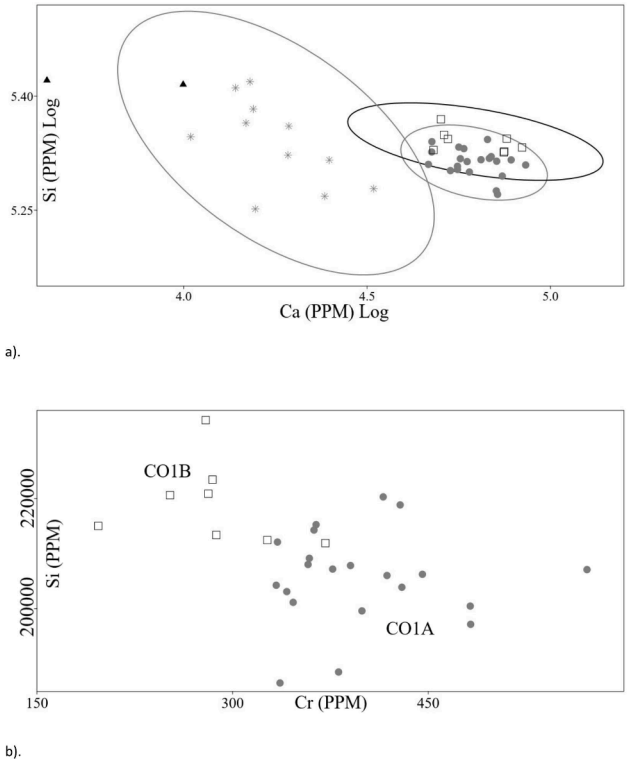

Fig. 6. (a). Contribution of quartz sands, represented in the chemical data most directly by Si, to groups CO1A (grey dot), CO1B (black square), CO2 (grey star), and CO3 (black triangle). Note group CO1A with the lowest overall amount of Si, with CO2 and CO3 having the highest amounts. (b) Further separation of subgroups CO1A and CO1B with pXRF, prepared as homogenized powders, using Cr and Si.

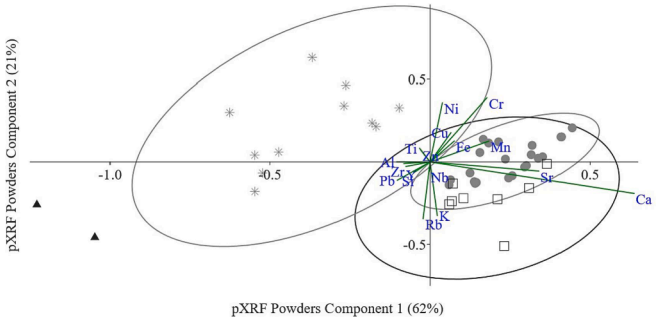

Fig. 7. Principle components analysis demonstrating low levels of Ca, Sr, K, Th, and Mn in group CO2, and high levels of Ti, Al, Zr, and Si (most samples) compared to CO1.

6. Results

6.1. Assessing precision of reference materials as powders and Pucks/Planchet-samples

To assess precision among the different analytical techniques and procedures, %RSD was calculated for each reference material and sample state. For the five powdered reference materials, 25 elements were able to be detected with LoDs below 33%. Of these elements detected, 20 had RSDs below 10%, and thus were precisely quantified with concentrations above the LoQ.

For the sixteen reference materials prepared as sherds and planchets, 23 elements were able to be detected, 19 had %RSDs near ten percent,

Table 10a-d
MANOVA demonstrating statistical separation of groups CO1A, CO1B, CO2, and CO3 for samples prepared and analyzed with pXRF as homogenized powders and analyzed with NAA only.

NAA Components 1 and 2

	CO1A	CO1B	CO2	CO3
CO1A		0.03	< 0.001	< 0.001
CO1B	0.03		< 0.001	< 0.001
CO2	< 0.001	< 0.001		< 0.001
CO3	< 0.001	< 0.001	< 0.001	

A). NAA MANOVA P- Values

Intact Sherds Components 1 and 2

	CO1A	CO1B	CO2	CO3
CO1A		0.09	< 0.001	< 0.001
CO1B	0.09		< 0.001	< 0.001
CO2	< 0.001	< 0.001		< 0.001
CO3	< 0.001	< 0.001	< 0.001	

B). Whole Sherds MANOVA P - Values

Powders Components 1 and 2

	CO1A	CO1B	CO2	CO3
CO1A		0.008	< 0.001	< 0.001
CO1B	0.008		< 0.001	< 0.001
CO2	< 0.001	< 0.001		< 0.001
CO3	< 0.001	< 0.001	< 0.001	

C). Homogenized Powders MANOVA P-Values

Planchets Data Components 1 and 2

	CO1A	CO1B	CO2	CO3
CO1A		0.25	< 0.001	< 0.001
CO1B	0.25		< 0.001	< 0.001
CO2	< 0.001	< 0.001		< 0.001
CO3	< 0.001	< 0.001	< 0.001	

D). Planchets MANOVA P - Values

MANOVA Parameters	NAA	Whole Sherds	Powders	Planchets
p-value*	< 0.001	< 0.001	< 0.001	< 0.001
Wilk's Lambda	0.1077	0.0573	0.3994	0.3899
df1	6	6	6	6
df2	74	74	74	74
F	25.25	39.09	49.38	49.38

*all p-values with Bonferroni Significance

MANOVA Parameters	NAA	Whole Sherds	Powders	Planchets
p-value*	< 0.001	< 0.001	< 0.001	< 0.001
Wilk's Lambda	0.1077	0.0573	0.3994	0.3899
df1	6	6	6	6
df2	74	74	74	74
F	25.25	39.09	49.38	49.38

*all p-values with Bonferroni Significance.

Table 11
T-test showing contribution of Si and Zr to the Coarse Orange groups, using the homogenized-powders dataset analyzed with pXRF.

Element	Si	Si	Zr	Zr
Comparison	CO1A - CO1B	CO1A – CO2	CO1A - CO1B	CO1A – CO2
K-S Test for Normality	Normal Distribution	Normal Distribution	Normal Distribution	Normal Distribution
Test for Sample Comparison	Equal Variance *t*-test	Equal Variance *t*-test	Equal Variance *t*-test	Equal Variance *t*-test
d.f.	27	30	27	30
Test Statistic	$t = -3.09$	$t = -2.12$	$t = -1.19$	$t = -4.46$
p-value	0.0005	0.04	0.24	0.0006

and thus precisely quantified. Comparison of the precision measured in the different techniques indicate that powder reference materials produce slightly lower %RSD values. Comparing the %RSD values for the four standards used in common to correct the pXRF across sample preparation techniques indicates that slightly more elements can be quantified with a higher precision among reference materials prepared as powders (Table 3).

6.2. Empirical Correction and assessing accuracy using reference materials

To validate the accuracy of the empirical corrections used for the different reference material preparation states, SRMs not used to construct the corrections were assayed. SRM2711a yielded 15 elements returning<10%Error compared to consensus values, and three elements returning<20%Error (Table 4). A cutoff of 20%Error was applied to filter out elements not accurately measured by the pXRF (following Dussubieux et al., 2007; Quinn et al., 2020). While Zr and Nb are not reported for SRM2711a, these elements have an acceptable %Error and %RSD in other reference materials and were thus included for further evaluation. A regression incorporating all 15 powdered reference materials demonstrates a high correlation among expected and observed values after correction (Fig. 2). Thus, seventeen elements were available for characterizing the powdered archaeological samples into chemical groups and appropriate for interlaboratory comparison.

Empirical correction of the sherd/planchet datasets was assessed using SRM2711 (Table 4). Fifteen elements yielded<10%Error, and two had errors between 10 and 20%; again, Zr and Nb were included despite consensus values not being reported. A regression utilizing the seventeen elements with an acceptable %RSD and %Error, across all 16 reference materials, demonstrate a high correlation among expected and observed values (Supplementary Materials 3). These same seventeen elements, used for the powder dataset also, were appropriate to characterize the sherd and planchet archaeological samples into chemical groups.

Comparing all elements reported for the four reference materials used to correct both the powdered and planchet datasets (Table 6), demonstrate that powders return the lowest %Error values overall, a

statistically significant outcome (Supplementary Materials 4a). When the 15 reported elements with an acceptable precision and accuracy are considered, this pattern remains. A *t*-test comparing %Error among samples prepared as powders and planchets again demonstrates a statistical difference in three of four reference materials (Table 7).

6.3. Linear dynamic range of Coarse Orange ceramics

To ensure that every Coarse Orange sample remained within the LDR, the %RSD of each sample was calculated using the replicate assays of archaeological samples for each of the three preparation techniques. Sherds were assayed five times each, while powders and planchets were assayed four times each.

For powdered samples, 20 elements had %RSD values below or near 10%, and within the LoQ. Ten elements (Al, Si, P, K, Ca, Ti, Fe, Rb, Sr, Zr) had an average %RSD less than one. Eight elements (V, Cr, Mn, Ni, Cu, Zn, Y, Nb) had an average %RSD between one and five. Two elements (Pb, Th) had an average %RSD between five and ten.

For comparison, in the planchets archaeological dataset, acceptable precision was achieved for 19 elements. Ten elements had an average % RSD value below or near one (Al, Si, P, K, Ca, Ti, Fe, Rb, Sr, Zr), nine had an average %RSD between one and five (V, Cr, Mn, Ni, Cu, Zn, Y, Nb), and none had a %RSD of 5–10.

For the sherd sample, nineteen elements had acceptable precision. No elements had an average %RSD value less than one. Thirteen elements (Al, Si, K, Ca, Ti, Fe, Cu, Zn, Rb, Sr, Y, Zr, Nb) had an average % RSD between one and five, and six elements (P, V, Cr, Mn, Ni, Pb) had an average %RSD between five and ten. Given their concentrations, Al, Si, K, Ca, Mn, and Fe should have precisions near or below one %RSD, because as concentration departs upward from the lower LoQ, precision increases systematically (Gustavo González et al., 2010; Schepers et al., 2004).

Thus, precision is significantly reduced in the sherds than in the powders and planchet-specimens. The combination of concentrations well above the lower LoQ, and comparatively low precision, indicates that this preparation method introduces errors into the analysis, hindering quantification. This observation is indicated with a chi-square test, as sherds offer the least precise results; and the powders dataset offers the highest precision (Supplementary Materials 4b).

After applying these validation procedures, we identified that 17 elements (Table 5) were within the Vanta's LDR and calibration range. Chemical group characterization of the archaeological datasets then occurred using these 17 validated elements.

6.4. Variability in the Coarse Orange dataset

Examining the %RSD values among the Coarse Orange dataset as a whole, and separately for each chemical group shows variability across sample preparation techniques (CO3 contained two samples and was excluded). Intact sherds contained the highest %RSD values for each element of the three preparation procedures in the Coarse Orange dataset as a whole, and for each chemical group (Table 8). Counting the elements with higher %RSD values among each of the differently prepared datasets indicate that the sherds dataset contains the highest amount of %RSD values, a statistically significant outcome (Supplementary Materials 4c). Preparing and analyzing samples as powders and planchets indicate the %RSD values among the powdered sample are the lowest overall. Similarly, a chi-square test demonstrates that the low % RSD values among the powder dataset are statistically significant in comparison to the planchet dataset. Including only the fifteen elements that share an acceptable %RSD among powders and planchets (Nb, Zr removed) yields similar results, with sherds having the highest %RSD (containing more variation), and powders having the lowest %RSD (less variation), as indicated by a chi-square test (Supplementary Materials 4d).

The greater variability presented by analysis of sherds over other sample preparation techniques likely derives from analytical error rather than either natural material composition or cultural variation in the production process. The high %RSD values in the sherds dataset are probably due to curved ceramic surfaces, inconsistent orientation, positioning at variable distances from the detector, an inhomogeneous ceramic body, variable particle sizes, and variable sampling locations. The lower %RSD among the powder dataset indicates less variation is detected because the aforementioned factors can be more easily controlled and consistently applied across repeated assays.

6.5. Interlaboratory comparisons of pXRF and NAA

Regression analysis involving fifteen elements measured by both pXRF and NAA was used to compare the concentrations obtained using each sample preparation technique to the values obtained with NAA. The weakest correlation was observed between the sherds and NAA (Table 9), suggesting that analysis of intact sherds using pXRF does not accurately quantify many elements and those data cannot be compared directly to other data collection techniques. Overall, the powders show the strongest correlation with NAA, likely due to a more uniform sample topography and sample homogeneity in comparison to sherds, producing more reliable and replicable results. When elements with a high % RSD and %Error are removed from all three datasets, powders still show the strongest correlation with NAA (Supplementary Materials 4e).

Further, SRM2711 (assayed 5 times by NAA) demonstrate that eleven elements (Al, K, Ca, Ti, Mn, Fe, Ni, Zn, Rb, Sr, Zr), yield lower % RSD values when assayed with pXRF compared to NAA (Table 4), and, in our case study, are more precisely measured using pXRF than NAA. Percent RSDs for elements Cr, V, As, Th, and Sb are lower as measured using NAA. These patterns of comparative instrumental precision for measuring elements in SRM2711 should be replicated in the measured variability of the Coarse Orange dataset.

6.6. Evaluating the capacity of pXRF to reproduce established chemical groups

The datasets for the three pXRF sample preparation techniques were used to evaluate the degree to which pXRF can independently reproduce chemical groups first identified using NAA (Stoner, 2013). Seventeen elements that had an acceptable precision and accuracy (near 10% RSD, <20% error) as powders and planchets were used to construct chemical groups of Coarse Orange pottery (Table 5). Eighteen elements were excluded because their values fell below an acceptable level of precision and accuracy among reference materials. Based on previous analysis (Stoner et al., 2008; Stoner and Glascock, 2012) data exploration began with a log-10 transformation, followed by a Principal Components Analysis (PCA) to determine which elements contributed the most variation to the dataset (Supplementary Materials 5a-c).

The PCA for each dataset indicated that PC1 was most strongly affected by elements Ca, Cr, Mn, and Sr; PC2 was most strongly affected by K, Cr, Ni, and Rb. Plotting the composition that resulted from measuring samples prepared through different techniques on Components 1 and 2, demonstrate separation of the 3 main groups (CO1, CO2, CO3) (Figs. 3a-c). Establishing the separation of sub-groups CO1A and CO1B is best achieved using measurements on samples in the powder dataset. This becomes clearer when group CO1 alone is plotted from data collected on sherds, powders, and planchets. The data generated from the powdered sample reproduced the clearest separation among subgroups based on bivariate scatter plots of Cr and Fe: two elements that are concentrated more highly in volcanic ash than in the clays. Data derived from the sherds dataset resulted in the least amount of separation (Figs. 4a-d).

While the three main chemical groups were distinguished using a hierarchical cluster analysis (HCA) (Figs. 5a-c), subgroups CO1A and CO1B were not clearly differentiated among any of the pXRF sample preparation techniques, nor the NAA dataset consisting of the same

sherds. A multivariate analysis of variance (MANOVA) using Components 1 and 2, did demonstrate a significant difference between all groups and subgroups (CO1A, CO1B, CO2, CO3) for the NAA dataset and the powdered pXRF dataset only (Table 10a,c). Subgroups CO1A and CO1B were not distinguished with MANOVA among the sherds and planchet datasets (Table 10b,d).

The influence of variable inclusions of quartz among CO1A, CO1B, and CO2 were examined using Si and Zr concentrations. A biplot of Cr and Si concentration values illustrates separation of subgroups CO1A and CO1B (Fig. 6a, b). A *t*-test indicates that when concentrations of Si and Zr are examined individually, a statistical difference exists across all groups (Table 11). However, Si does not account for all the variation between groups CO1A, CO1B, and CO2. Instead, Al, Ti, and Zr are also relatively high while Ca, Sr, and K are relatively low in group CO2 (Fig. 7) (also Pool, 1990).

7. Discussion and conclusion

The pXRF analysis in this study demonstrates that the same groups and subgroups identified previously through NAA can be reproduced, and subregional production recipes of Coarse Orange pottery differentiated. The study, therefore, provides validation for the use of recent generations of pXRF analyzers for compositional sourcing of archaeological pottery.

Statistical separation of subgroups CO1A and CO1B using pXRF data was only possible with samples prepared as powders, though even among the NAA chemical data, these subgroups are only subtly distinguished. Given that CO1B ceramics have a statistically higher amount of Si and Zr than group CO1A ceramics, the proportion of quartz to volcanic ash in those CO1B ceramics may be interpreted to be higher than in CO1A ceramics (Table 11). These new pXRF data therefore suggest that the slightly lower transition metal composition found in CO1B ceramics also resulted from dilution from a higher quartz fraction. Being able to measure Si directly, therefore, helps to develop a nuanced understanding of the compositional differences among the reference groups not previously identified among the NAA data.

Multiple assays of reference materials is necessary to determine precision, LoD, LoQ, accuracy, and LDR in achieving proper validation of calibrations or corrections, these quality control procedures should be applied to any instrument before analysis of unknown samples. Applying such protocols to our sample of Coarse Orange pottery lead us to several significant conclusions. (1) At least seventeen elements could be precisely and accurately quantified in the reference materials and archaeological samples. (2) The validation and correction of reference materials in our case study indicate that powdered standards offer better precision and accuracy than planchet standards (without a vacuum/He-flush atmosphere). (3) The averaged concentration derived from analysis at multiple locations on sherds failed to produce precise and accurate results that are comparable with NAA. This is attributable to both sherd heterogeneity and that the movement of sampling locations to create an averaged bulk estimate adding variability in the positioning of the sample relative to the detector. (4) Analysis of archaeological ceramics prepared as powders produced accurate and precise results comparable to NAA for many elements (c.f. LeMoine and Helperin, 2021). Proper validation requires replicate assays of unknown analytes to determine if obtained concentrations are precise, within the LoQ, and within the LDR, to produce accurately calibrated or corrected datasets. Utilizing such methods indicate that pXRF analysis can be used for independent analysis of Coarse Orange ceramic fabrics from the Tuxtlas Region of Southern Veracruz, and possibly elsewhere.

CRediT authorship contribution statement

Marc D. Marino: Conceptualization, Formal analysis, Writing – original draft, Writing – review & editing, Resources, Funding acquisition, Data curation, Investigation. **Wesley D. Stoner:** Conceptualization, Writing – original draft, Writing – review & editing, Funding acquisition, Resources, Supervision. **Lane F. Fargher:** Methodology, Validation, Writing – review & editing, Supervision. **Michael D. Glascock:** Methodology, Supervision, Funding acquisition, Resources.

Declaration of Competing Interest

The authors declare that they have no known competing financial interests or personal relationships that could have appeared to influence the work reported in this paper.

Acknowledgements:

Support for this research was provided by NSF grant 1912776 to the Archaeometry Laboratory at MURR. The Sturgis International Fellowship is also thanked for providing funds for this research. We wish to thank all anonymous reviewers for their helpful counterpoints and commentary that significantly pushed us to improve this manuscript.

Availability of data

The data that supports the findings of this study are available in the supplementary material of this article.

Appendix A. Supplementary data

Supplementary data to this article can be found online at https://doi.org/10.1016/j.jasrep.2021.103315.

References

Aimers, Jim J., Farthing, Dori J., Shugar, Aaron N., 2012. Handheld XRF Analysis of Maya Ceramics: A Pilot Study Presenting Issues Related to Quantification and Calibration. In: Shugar, Aaron, Mass, Jennifer L. (Eds.), Handheld XRF For Art and Archaeology. Leuven University Press, Belgium, pp. 423–448. https://doi.org/10.2307/j.ctt9qdzfs.17.

Arnold, Dean E., 1985. Ceramic Theory and Culture Process. Cambridge University Press, Cambridge.

Arnold, Dean E., 2000. Does Standardization of Ceramic Paste Really Mean Anything? J. Archaeol. Meth. Theor. 7 (4), 333–375. https://doi.org/10.1023/A:1026570906712.

Arnold, Dean E., Neff, Hector, Bishop, Ronald L., 1991. Compositional Analysis and "Sources" of Pottery: An Ethnoarchaeological Approach. Am. Anthropol. 93 (1), 70–90. https://doi.org/10.1525/aa.1991.93.1.02a00040.

Arnold, Phillip J., Pool, Christopher A., Kneebone, Ronald R., Santley, Robert S., 1993. Intensive Ceramic Production and Classic-Period Political Economy in the Sierra De Los Tuxtlas, Veracruz, Mexico. Ancient Mesoamerica 4, 175–191. https://doi.org/10.1017/S0956536100000870.

Bishop, Ronald L. 1980. Aspects of Ceramic Compositional Modelling. In Models and Methods in Regional Exchange. Edited by R. E. Fry. Society for American Archaeology, *SAA Papers 1*. Pp. 47-66.

Blackman, M James, Bishop, Ronald L., 2007. The Smithsonian–NIST Partnership: the Application of Instrumental Neutron Activation Analysis to Archaeology. Archaeometry 49, 321–341. https://doi.org/10.1111/j.1475-4754.2007.00304.x.

Boulanger, Matthew T., Fehrenbach, S.S., Glascock, Michael D., 2012. Experimental Evaluation of Sample-Extraction Methods and the Potential for Contamination in Ceramic Specimens. Archaeometry 2013, 880–892.

Carpenter, Andrea J., Feinman, Gary M., 1999. The Effects of Behavior on Ceramic Composition: Implications for the Definition of Production Locations. J. Archaeol. Sci. 26, 783–796. https://doi.org/10.1006/jasc.1998.0347.

Desroches, Dany, Paul Bédard, L., Lemieux, Simone, Esbensen, Kim H., 2018. Suitability of Using a Handheld XRF for Quality Control of Quartz in an Industrial Setting. Miner. Eng. 126, 36–43. https://doi.org/10.1016/j.mineng.2018.06.016.

Dussubieux, Laure, Mark Golitko, Patrick Ryan Williams, and Robert J. Speakman 2007. Laser Ablation-Inductively Coupled Plasma-Mass Sepctrometery Analysis Applied to the Characterization Peruvian Wari Ceramics. In *Archaeological Chemistry: Analytical Techniques and Archaeological Interpretation.* Edited by, Michael D. Glascock, Robert J. Speakman, and Rachel S. Popelka-Filcoff, Pp. 349-375, Oxford University Press, Oxford. https://doi.org/10.1021/bk-2007-0968.ch019.

Forster, Nicola, Grave, Peter, Vickery, Nancy, Kealhofer, Lisa, 2011. Non-Destructive Analysis using PXRF: Methodology and Application to Archaeological Ceramics. X-Ray Spectrom. 40, 389–398. https://doi.org/10.1002/xrs.1360.

Frahm, Ellery, 2017. First Hands-On Tests of an Olympus Vanta Portable XRF Analyzer to Source Armenian Obsidian Artifacts. Int. Assoc. Obsidian Stud. Bull. 58, 8–23.

Frahm, Ellery, 2018. Ceramic Studies Using Portable XRF: From Experimental Tempered Ceramics to Imports and Imitations at Tell Mozan, Syria. J. Archaeol. Sci. 90, 12–38. https://doi.org/10.1016/j.jas.2017.12.002.

Glascock, Michael D. 1992. Characterization of Archeological Ceramics at MURR by Neutron Activation Analysis and Multivariate Statistics. In *Chemical Characterization of Ceramic Pastes in Archaeology*, edited by Hector Neff, pp. 11-26. Prehistory Press, Madison.

Glascock, Michael D. 2020. Tables to Support the Analytical Methods Used at MURR: NAA, XRF and ICP-MS. University of Missouri Research Reactor, Columbia, Missouri. https://archaeometry.missouri.edu/downloads/Tables%20to%20Support%20Analytical%20Methods%20in%20Use%20at%20MURR.pdf.

Glascock, Michael D., 2017. Determination of Elements in Clays and Standard Reference Materials. Report on file. Archaeometry Laboratory. University of Missouri Research Reactor.

Glascock, Michael D., Neff, Hector, 2003. Neutron Activation Analysis and Provenance Research in Archaeology. Meas. Sci. Technol. 14, 1516–1523. https://doi.org/10.1088/0957-0233/14/9/304.

Golitko, Mark, John Dudgeon, Hector Neff, and John Terrell 2012. Identification of Post-Depositional Chemical Alteration of Ceramics from the North Coast of Papua New Guinea (Sanduan Province) By Time-of-Flight-Laser Ablation-Inductively Coupled Plasma-Mass Spectrometry (TOF-LA-ICP-MS). *Archaeometry* 54. 80-100. https://doi.org/10.1111/j.1475-4754.2011.00612.x.

Gustavo González, A., Ángeles Herrador, M., Asuero, Agustín G., 2010. Intra-Laboratory Assessment of Method Accuracy (Trueness And Precision) by Using Validation Standards. Talanta 82 (5), 1995–1998. https://doi.org/10.1016/j.talanta.2010.07.071.

Hu, Bifeng, Chen, Songchao, Jie, Hu, Xia, Fang, Junfeng, Xu, Li, Yan, Shi, Zhou, 2017. Application of Portable XRF and VNIR Sensors for Rapid Assessment of Soil Heavy Metal Pollution. PLoS One 12 (2), 1–13. https://doi.org/10.1371/journal.pone.0172438.

Hunt, Alice M., Speakman, Robert J., 2015. Portable XRF Analysis of Archaeological Sediments and Ceramics. J. Archaeol. Sci. 53, 626–638. https://doi.org/10.1016/j.jas.2014.11.031.

Jang, Mia, 2010. Application of Portable X-ray Fluorescence (pXRF) for Heavy Metal Analysis of Soils in Crop Fields Near Abandoned Mine Sites. Environ. Geochem. Health 32, 207–216. https://doi.org/10.1007/s10653-009-9276-z.

JCGM - BIPM, IEC, IFCC, ILAC, IUPAC, IUPAP, ISO, OIML 2012. The International Vocabulary of Metrology—Basic and General Concepts and Associated Terms (VIM), 3rd edn. JCGM 200:2012. https://www.bipm.org/documents/20126/2071204/JCGM_200_2012.pdf/f0e1ad45-d337-bbeb-53a6-15fe649d0ff1.

Johnson, Jack, 2014. Accurate Measurements of Low Z Elements in Sediments and Archaeological Ceramics Using Portable X-ray Fluorescence (PXRF). J. Archaeol. Meth. Theor. 21, 563–588. https://doi.org/10.1007/s10816-012-9162-3.

Killion, Thomas W., Urcid, Javier, 2001. The Olmec Legacy: Cultural Continuity in Mexico's Southern Gulf Coast Lowlands. J. Field Archaeol. 28 (1 and 2), 3e25. https://doi.org/10.2307/3181457.

Lemier, Bruno, 2018. A Review of pXRF (field portable X-ray fluorescence) Applications for Applied Geochemistry. J. Geochem. Explor. 188, 350–363. https://doi.org/10.1016/j.gexplo.2018.02.006.

May, Willie E., Reenie M. Parris, Charles M. Beck, John D. Fasset, Robert R. Greenberg, Franklin R. Guenther, Gary W. Kramer, Stephen Wise, Thomas E. Gills, Jennifer C. Colbert, Robert J. Gettings, and Bruce S. MacDonald. 2000. Definitions of Terms and Modes Used at NIST for Value-Assignment of Reference Materials for Chemical Measurements. *NIST Special Publications 260-136: Standard Reference Materials.* U.S. Government Printing Office, Washington D.C. https://www.nist.gov/system/files/documents/srm/SP260-136.PDF.

McCormick, David. R., and E. Christian Wells, 2014. Pottery, People, and pXRF: Toward the Development of Compositional Profiles for Southeast Mesoamerican Ceramics. In S. L. Lopez Varela (Ed.), *Social Dynamics of Ceramic Analysis: New Techniques and Interpretations: Papers in Honour of Charles C. Kolb*, pp. 22-35. BAR International Series 2683. ISBN 978 1 4073 1329 0.

Neff, Hector 2000. Neutron Activation Analysis for Provenance Determination in Archaeology. In *Modern Analytical Methods in Art and Archaeology*, edited by E. C. a. G. Spoto, pp. 81-134. John Wiley and Sons, Inc., NY.

Neff, H., Bishop, R.L., Sayre, E.V., 1988. A Simulation Approach to the Problem of Tempering in Compositional Studies of Archaeological Ceramics. J. Archaeol. Sci. 15 (2), 159–172. https://doi.org/10.1016/0305-4403(88)90004-0.

Pool, Christopher A. 1990. *Ceramic Production, Resource Procurement, and Exchange at Matacapan, Veracruz, Mexico*. Doctoral Dissertation, Department of Anthropology, Tulane University, New Orleans. https://digitallibrary.tulane.edu/islandora/object/tulane:24629.

Pool, Christopher A. and Wesley D. Stoner 2008. But Robert, Where did the Pots Go? Ceramic Exchange and the Economy of Ancient Matacapan. *Journal of Anthropological Research* 64(3):411-423. https://www.jstor.org/stable/20371264.

Quinn, P., Yang, Y., Xia, Y., Li, X., Ma, S., Zhang, S., Wilke, D., 2020. Geochemical Evidence for the Manufacture, Logistics, and Supply-Chain Management of Emperor Qin Shihuang's Terracotta Army, China. Archaeometry 63 (1), 40–52. https://doi.org/10.1111/arcm.12613.

Rye, Owen S. 1981. Pottery Technology: Principles and Reconstruction. Taraxacum.

Santley, Robert S., Phillip J. Arnold, and Christopher Pool 1989. The Ceramic Production System at Matacapan, Veracruz, Mexico. J. Field Archaeol. 16(1):107-132.

Sayre, Edward V. and Garman Harbottle 1979. The Analysis by Neutron Activation of Archaeological Ceramics Related to Teotihuacan: Local Wares and Trade Sherds. In Brookhaven National Laboratory, Informal Report C-2250.

Schepers, Ute, Ermer, Joachim, Preu, Lutz, Wätzig, Hermann, 2004. Wide Concentration Range Investigation of Recovery, Precision and Error Structure in Liquid Chromatography. J. Chromatogr. B 810 (1), 111–118. https://doi.org/10.1016/j.jchromb.2004.07.023.

Scott, Rebecca. B., Bert Neyt, Corinne Hofman, and Patrick Degryse 2018. Determining the Provenance of Cayo Pottery From Grenada, Lesser Antilles, Using Portable X-Ray Fluorescence Spectrometry. *Archaeometry* 60(5):966-985. https://doi.org/10.1111/arcm.12359.

Shackley, M. Steven 2011. An Introduction to X-Ray Fluorescence (XRF) Analysis in Archaeology. In *X-Ray Fluorescence Spectrometry (XRF) in Geoarchaeology*. Edited by M. S. Shackley, pp. 7-44. Springer Press, New York. https://doi.org/10.1007/978-1-4419-6886-9_2.

Speakman, Robert J. 2012. Evaluation of Bruker's Tracer Family Factory Obsidian Calibration for Handheld Portable XRF Studies of Obsidian. Prepared by: Center for Applied Isotope Studies, University of Georgia. *Report Prepared for Bruker AXS, Kennewick, Washington.*.

Speakman, Robert J., Shackley, Steven M., 2013. Silo Science and Portable XRF in Archeology: A Response to Frahm. J. Archaeol. Sci. 40, 1435–1443.

Stoner, Wesley D. 2002. Coarse Orange Pottery Exchange in Southern Veracruz: A Compositional Perspective on Centralized Craft Production and Exchange in the Classic Period. M.A. thesis, Department of Anthropology, University of Kentucky, Lexington, KY. https://uknowledge.uky.edu/gradschool_theses/187.

Stoner, Wesley D. 2011. Disjuncture among Classic Period Cultural Landscapes in the Tuxtla Mountains, Southern Veracruz, Mexico. Ph.D. Dissertation, Department of Anthropology, University of Kentucky, Lexington. https://uknowledge.uky.edu/gradschool_diss/35.

Stoner, Wesley D., 2013. Interpolity Pottery Exchange in the Tuxtla Mountains, Southern Veracruz, Mexico. Latin Am. Antiquity 24 (3), 262–288. https://doi.org/10.7183/1045-6635.24.3.262.

Stoner, Wesley D., 2016. The Analytical Nexus of Ceramic Paste Compositional Studies: A Comparison on NAA, LA-ICP-MS, and Petrography in the Prehispanic Basin of Mexico. J. Archaeol. Sci. 76, 31–47. https://doi.org/10.1016/j.jas.2016.10.006.

Stoner, Wesley D., Glascock, Michael D., 2012. The Forest or the Trees? Behavioral and Methodological Considerations for Geochemical Characterization of Heavily Tempered Ceramic Pastes Using NAA and LA-ICP-MS. J. Archaeol. Sci. 39, 2668–2683. https://doi.org/10.1016/j.jas.2012.04.011.

Stoner, Wesley D., Pool, Christopher A., 2015. The Archaeology of Disjuncture: Classic Period Disruption and Cultural Divergence in the Tuxtla Mountains of Mexico. Curr. Anthropol. 56 (3), 385–420. https://doi.org/10.1086/681524.

Stoner, Wesley D., Shaulis, Barry J., 2021. Chemical Mapping to Evaluate Post-Depositional Diagenesis Among the Earliest Ceramics in the Teotihuacan Valley, Mexico. Minerals 11 (4), 1–28. https://doi.org/10.3390/min11040384.

Stoner, Wesley D., Millhauser, John K., Rodríguez-Alegría, Enrique, Overholtzer, Lisa, Glascock, Michael D., 2013. Taken with a Grain of Salt: Experimentation and the Chemistry of Archaeological Ceramics from Xaltocan, Mexico. J. Archaeol. Meth. Theor. 21 (4), 862–898. https://doi.org/10.1007/s10816-013-9179-2.

Stoner, Wesley D., Pool, Christopher A., Neff, Hector, Glascock, Michael D., 2008. Exchange of Coarse Orange Pottery in the Middle Classic Tuxtla Mountains, Southern Veracruz, Mexico. J. Archaeol. Sci. 35 (5), 1412–1426. https://doi.org/10.1016/j.jas.2007.10.008.

Taverniers, Isabel, De Loose, Marc, Van Bockstaele, Erik, 2004. Trends in Quality in the Analytical Laboratory. II. Analytical Method Validation and Quality Assurance. TrAC, Trends Anal. Chem. 23 (8), 535–552. https://doi.org/10.1016/j.trac.2004.04.001.

Thomsen, Volker, 2007. Basic Fundamental Parameters in X-ray Fluorescence. Spectroscopy 22 (5), 46–50.

Thomsen, Volker, Schatzlein, Debbie, Mercuro, David, 2003. Limits of Detection in Spectroscopy. Spectroscopy 18 (12), 112–115.

Weigand, Phil C., Harbottle, Garman, Sayre, Edward V., 1977. Turquoise Sources and Source Analysis: Mesoamerica and the Southwestern U.S.A. In: Earle, T.K., Ericson, J.E. (Eds.), Exchange Systems in Prehistory. Academic Press, New York, pp. 15–32. https://doi.org/10.1016/B978-0-12-227650-7.50008-0.

Xu, Wengpeng, Niziolek, Lisa C., Feinman, Gary M., 2019. Sourcing Gingbai Porcelains from the Java Sea Shipwreck: Compositional Analysis Using Portable XRF. J. Archaeol. Sci. 103, 57–71. https://doi.org/10.1016/j.jas.2018.12.010.